Research Article

Wei Li and Chengping Zhang*

Stability Analysis of a Slurry Trench in **Cohesive-Frictional Soils**

https://doi.org/10.1515/geo-2019-0069 Received Jan 22, 2019; accepted May 31, 2019

Abstract: The slurry trench has become increasingly common in underground engineering and the stability of a slurry trench has been an important design issue. Although many studies have focused on the overall stability of a slurry trench, few of that are related to its local stability. Based on the limit analysis, both two dimensional and three dimensional rotational failure mechanisms for the local failure of a slurry trench in a sandwiched weak layer are proposed, and the upper solutions of 2D and 3D safety factors for local failure mechanisms are derived to evaluate the stability of a slurry trench. Moreover, a numerical analysis combined with the strength reduction technique is performed to investigate the local stability and the local failure process of a slurry trench. The proposed analytical method is verified through the comparison with the results of FLAC3D. Finally, a parametric study on the influences of geometric and geologic parameters on the local stability of the slurry trench are investigated. The results show that the investigation on the local stability of a slurry trench is effective and reasonable, which can provide a reference for the engineers in the practical engineering.

Keywords: Limit analysis; Slurry trench; Local stability; Numerical simulation; Safety factor

1 Introduction

A slurry trench is built for some reinforced concrete aphragm walls surrounding tunnels and open cuts to lay

walls such as cut-off walls adjacent to groundwater or di-

*Corresponding Author: Chengping Zhang: Key Laboratory of Urban Underground Engineering of the Education Ministry, Beijing Jiaotong University Beijing 100044, China; School of Civil Engineering, Beijing Jiaotong University, Beijing 100044, China; Email: chpzhang@bitu.edu.cn

Wei Li: Key Laboratory of Urban Underground Engineering of the Education Ministry, Beijing Jiaotong University Beijing 100044, China; School of Civil Engineering, Beijing Jiaotong University, Beijing 100044, China

foundations. A slurry trench has become increasingly common in underground engineering. Therefore, the stability of a slurry trench is an important design issue. There are typically two kinds of slurry trench failure, namely the overall and local failure. The overall failure tends to occur at the shallow layer of soil and then the failure zone propagates to the ground surface leading to the failure of slurry trench. While there is a relatively weak layer below the ground surface, the local failure of the weak layer would occur and influence the stability of the slurry trench, which could cause the unstable soil to flow into the slurry trench inducing lateral extrusion of the trench wall, even causing damage to the nearby architectural structure and buried pipelines, as shown in Figure 1.

There have been several methods adopted to investigate the overall stability of a slurry trench. For good re-



Figure 1: Concrete overflow caused by local failure of a slurry trench.

producibility, numerical simulations have been performed to investigate the stability of a slurry trench and visualize the failure zone [1-4]. The limit equilibrium analysis methods investigate the bearing capacity problem by presupposing a failure mechanism and considering the static equilibrium of the failure zone [5-11]. Different influence factors of slurry trench are considered in these references. Moreover, Han et al. [12, 13] attempted to adopt the limit analysis to study the stability of a slurry trench for 2D and 3D failure mechanisms.

However, the references above mainly pay attention to the overall stability of a slurry trench but neglect the local stability of a slurry trench, which is also easy to occur when the geological condition is a weak soil layer sandwiched between two relatively stronger layers. In this case, the failure zone develops in the weak layer of the soil, and then the soil of weak layer near the trench wall will fall off and bury the slurry trench, which could severely affect the safety of engineering and cost more subsequent construction effort. With regard to the local stability of slurry trench, Tsai et al. [14, 15] and Shen [16] studied the problem of local stability of sandwiched weak soil in a slurry trench by adopting the limit equilibrium method to analyse the stress distribution on the trench surface. Xiao and Sun [10] investigate the local stability of a slurry trench through the centrifuge model test and found that the slurry trench is prone to a local failure in a sandwiched weak soil. It is worth noting that Han et al. [13] proposed the local failure mechanism of a slurry trench based on the limit analysis, but their work is limited in the purely cohesive soil.

In this paper, the purpose is to adopt the limit analysis to develop a 2D and 3D local stability analysis of a slurry trench in a cohesive-frictional soil (weak layer) sandwiched by two relatively stronger soils. And a formula to determine the safety factor of local stability of a slurry trench is derived to obtain the upper bound solution. Besides, a numerical method combined with the strength reduction technique is presented to study the local stability of a slurry trench. Through the comparisons of results between the numerical method and analytical solution, the effectiveness and reasonability of the analytical approach is verified. Finally, a parametric study of the influence on the safety factor is carried out.

2 Limit Analysis for Local Stability of a Slurry Trench in **Cohesive-Frictional Soils**

The main advantages of limit analysis lie in its simplicity and rigorous theoretical basis considering the stressstrain relationship of soils without a prior assumption on the failure surface and stress distribution. There have been a number of research investigations related to the application of limit analysis to the slopes and tunnels, and it is shown that studies based on limit analysis have provided satisfactory results [17–27]. Therefore, this paper intends to apply the limit analysis to the local stability of a slurry trench. 2D and 3D rotational local failure mechanisms of a slurry trench suitable for cohesive-frictional soil (cohesivefrictional soil $c \neq 0 \varphi \neq 0$, purely cohesive soil $\varphi = 0$, and purely frictional soil c = 0) are presented.

In order to follow the limit analysis theory, some assumptions must be made to simplify the complicated field conditions of a slurry trench into explicit theoretical model:

First, a kinematically admissible velocity field is assumed to satisfy the normal flow rule (equal dilatancy and friction angles $\psi = \varphi$) associated with the yield condition of the soil and the boundary condition of the failure mechanism, and the Mohr-Coulomb yield criterion is applied in the analysis. The associated flow rule requires the following relationship among the principal strain rates in the 3D analysis:

$$\dot{\varepsilon}_1 + \dot{\varepsilon}_2 + \dot{\varepsilon}_3 + (\dot{\varepsilon}_1 - \dot{\varepsilon}_2 - \dot{\varepsilon}_3) \sin \varphi = 0 \tag{1}$$

Where $\dot{\varepsilon}_1$, $\dot{\varepsilon}_2$, $\dot{\varepsilon}_3$ are principal strain rates and φ is the frictional angle.

Second, the thyxotropy of the slurry is assumed to make itself solidify and form a "cake" on the interface between the soil and slurry to prevent the fluid percolation in the soil. So the slurry and the underground water (if there is underground water) exerts a triangular hydrostatic pressure on the trench face, respectively.

Third, the local failure of a slurry trench is confined to a weak soil layer sandwiched by two stiff soils, the problem schematic is defined in Figure 2.

The dissipation rate W_D is calculated as the summation of the dot product of the elementary area and the velocity, as follows:

$$W_D = c \cdot \cos \varphi \int_{S_r} v_i dS_i \tag{2}$$

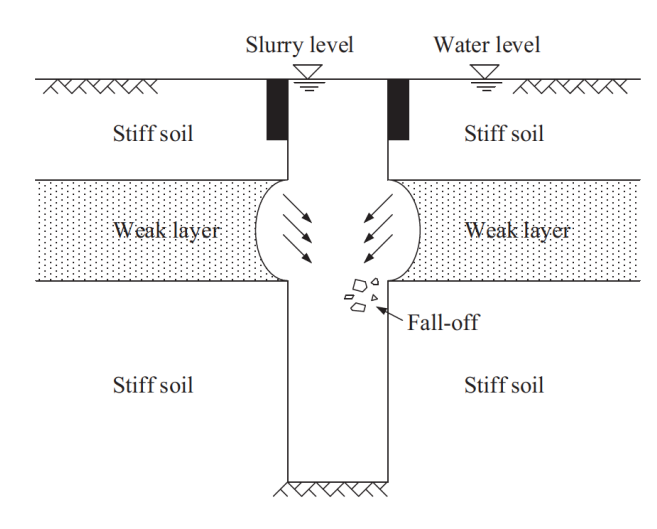


Figure 2: Problem definition.

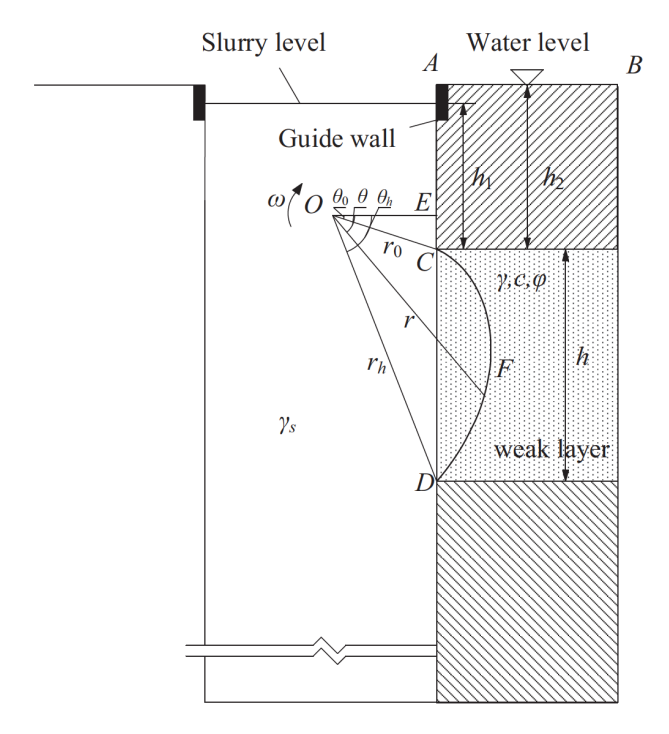


Figure 3: 2D rotational mechanism schematic for the local failure of a slurry trench.

where c is the cohesion, S_t is the discontinuity surface surrounding the failure mechanism of slurry trench. v_i is the velocity vector of elementary area dS_i .

The work rate done by the soil weight W_G is calculated as the summation of the dot product of the elementary block weight and the velocity, as follows:

$$W_G = \int_V \gamma_i \nu_i dV_i \tag{3}$$

where γ_i and v_i is respectively the unit weight and the vertical component of velocity of elementary block dV_i .

The work rate of the slurry pressure W_{sr} is calculated as the summation of the dot product of the slurry pressure of the elementary area and the velocity, as follows:

$$W_{Sr} = \int_{S_{in}} P_{Sri} v_i dS_i \tag{4}$$

where P_{sri} is the slurry pressure on the elementary area dS_i , v_i is the horizontal component of velocity, S_{in} is the interface between the soil and slurry.

If there is underground water in the soil, the parameters c, φ and γ above would be replaced by the effective cohesion c', effective friction angle φ' and the effective unit weight γ' , respectively. The work rate done by the hydrostatic pressure W_w on the trench face is calculated as follows:

$$W_W = \int_{S_{in}} P_{wi} \nu_i dS_i \tag{5}$$

where P_{wi} is the water pressure.

In this paper, the safety factor *F* of local stability of a slurry trench with given geometric parameters is defined as follows:

$$F = \frac{W_D + (W_{sr} - W_w)}{W_G} \tag{6}$$

Eq. (6) is a common way to define the safety factor as the ratio of the load-resisting capacity to the destructive effect [12, 13, 26, 28, 29]. The minimum value of the safety factor F can be achieved by numerically optimization with the help of the optimization tool implemented in the Matlab. The process uses an arbitrary user-defined set of the independent parameters as the starting point of the optimization and converges to a unique optimum by a sequence of computations.

2.1 2D Limit Analysis for Local Stability

The 2D local failure schematic of a slurry trench with a geology condition that a weak layer $(c-\varphi)$ is sandwiched between two relatively stronger layers is shown in Figure 3. A local failure develops inside the weak layer with a thickness of h. And the weak layer is h_1 below the slurry level and h_2 below the water level. The proposed 2D failure mechanism for the local stability of a slurry trench involves a rotational movement of a single rigid block, enveloped by a curve and defined by a logarithmic-spiral. The curve CFD is a surface of the velocity discontinuity rotating about the centre O, with an angular velocity ω . Note that r_0 , r_h , θ_0 , θ_h , can be easily identified from Figure 3. A set of parameters are related to θ_0 and θ_h . Hence, the rotational failure mechanism and the velocity field are entirely defined by

 θ_0 and θ_h . The expression of *r* is described as follows:

$$r = r_0 \cdot e^{(\theta - \theta_0) \tan \varphi} \tag{7}$$

where θ is the angle with *OE*.

The work rate of the soil weight is calculated as the dot product of the soil weight of *CFD* and the vertical component of the velocity at the centroid. According to the centroid formula of the combined figure:

$$\begin{cases} x_c = \frac{\sum A_i \cdot x_i}{\sum A_i} \\ y_c = \frac{\sum A_i \cdot y_i}{\sum A_i} \end{cases}$$
 (8)

Therefore, the work rate of soil weight W_G of CFD is calculated as follows:

$$W_{G} = \gamma \cdot A_{CFD} \cdot \omega \cdot x_{c}^{CFD} = \gamma \omega (A_{OCFD} \cdot x_{c}^{OCFD})$$

$$+ A_{OCE} \cdot x_{c}^{OCE} - A_{OED} \cdot x_{c}^{OED})$$

$$= \gamma \omega \left(\int_{\theta_{0}}^{\theta_{h}} \frac{1}{2} r^{2} \cdot \frac{2}{3} r \cos \theta d\theta + \frac{1}{2} r_{0} \sin \theta_{0} \cdot r_{0} \cos \theta_{0} \cdot \frac{2}{3} r_{0} \cos \theta_{0} - \frac{1}{2} r_{h} \sin \theta_{h} \cdot r_{h} \cos \theta_{h} \cdot \frac{2}{3} r_{0} \cos \theta_{0} \right)$$

$$(9)$$

where A_{CFD} and x_c^{CFD} are the area of the *CFD* and the horizontal coordinate of the centroid of *CFD*. Similarly, the A_{OCFD} , A_{OCE} and A_{OED} are the areas of *OCFD*, *OCE* and *OED*, respectively. And the x_c^{OCFD} , x_c^{OCE} and x_c^{OED} are the horizontal coordinates of the centroid of *OCFD*, *OCE* and *OED*, respectively. r_0 and r_h are the functions of θ_0 and θ_h , as follows:

$$\begin{cases} r_0 = h/(-\sin\theta_0 + \cos\theta_0 \tan\theta_h) \\ r_h = h/(\sin\theta_h - \cos\theta_h \tan\theta_0) \end{cases}$$

The elementary area *dS* along the discontinuity surface *CFD* is as follows:

$$dS = \frac{rd\theta}{\cos \varphi} \tag{10}$$

According to Eq. (2), the dissipation is calculated as the integration along the discontinuity surface *CFD*, as follows:

$$W_D = c\omega \int_{\theta_D}^{\theta_h} r^2 d\theta \tag{11}$$

The slurry pressure on the any point of interface *CD* is as follows:

$$P_{sr} = \gamma_{sr} \left(h_1 - r_0 \sin \theta_0 + r_0 \cos \theta_0 \tan \theta \right) \tag{12}$$

where γ_{sr} is the unit weight of slurry in the trench.

The elementary area *dS* along the interface *CD* is as follows:

$$dS = \frac{r_0 \cos \theta_0}{\cos^2 \theta} d\theta \tag{13}$$

According to Eq. (4), the work rate done by the slurry pressure W_{sr} is calculated along the interface CD, as follows:

$$W_{sr} = \gamma_{sr}\omega \int_{\theta_0}^{\theta_h} (h_1 - r_0 \sin \theta_0) + r_0 \cos \theta_0 \tan \theta \frac{r_0^2 \cos^2 \theta_0}{\cos^2 \theta} \tan \theta d\theta$$
(14)

Similarly, the possible work rate done by the hydrostatic water pressure on the trench face *CD* is calculated as follows:

$$W_{w} = \gamma_{w}\omega \int_{\theta_{0}}^{\theta_{h}} (h_{2} - r_{0}\sin\theta_{0})$$

$$+r_{0}\cos\theta_{0}\tan\theta \frac{r_{0}^{2}\cos^{2}\theta_{0}}{\cos^{2}\theta}\tan\theta d\theta$$
(15)

Where γ_W is the unit weight of water.

Hence, the safety factor F can be obtained by substituting the Eqs. (9), (11), (14) and (15) into the Eq. (6), which depends on the angle parameters θ_0 and θ_h . A least upper bound solution can be found by numerically optimizing Eq. (6) with respect to θ_0 and θ_h .

2.2 3D Limit Analysis for Local Stability

In this section, a 3D rotational local failure mechanism in cohesive-frictional soils is presented. The mechanism has a horn shape with an apex angle 2φ , and only a portion of this mechanism intersects with the weak layer of a slurry trench, as shown in Figure 4. The mechanism has one symmetric plane on the (x, z) plane. The trace of the mechanism (discontinuity surface) on the vertical symmetry plane is defined by two log spirals CD and C'D'.

$$\begin{cases} r = r_0 \cdot e^{(\theta - \theta_0) \tan \varphi} \\ r' = r'_0 \cdot e^{-(\theta - \theta_0) \tan \varphi} \end{cases}$$
 (16)

where r is distance of the point on the log spiral CD to the origin O(r') represent the distance of the point of C'D'). r_0 and r_h are the length of OC and OD, respectively. Similarly, r'_0 and r'_h are the length of OC' and OD'.

The mechanism can be regarded as being generated by rotating a circle of increasing diameter (shaded circle in Figure 4) about an axis passing through point *O* outside

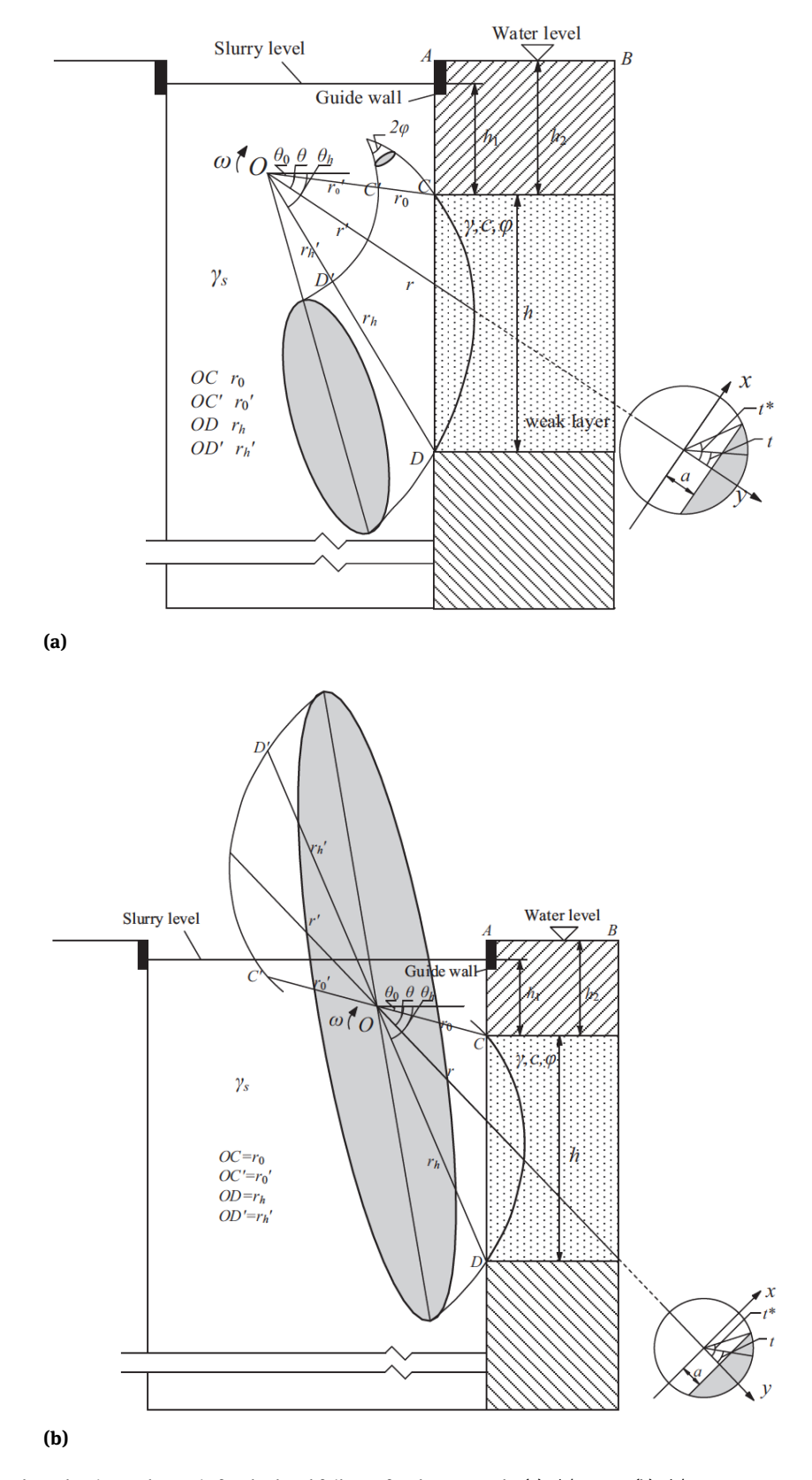


Figure 4: 3D rotational mechanism schematic for the local failure of a slurry trench: (a) $r_0'/r_0 > 0$; (b) $r_0'/r_0 < 0$.

the circle. When the circle is rotated about an axis passing through the circle ($r'_0/r_0 < 0$), the failure mechanism is transformed into the case in Figure 4(b) and the C'D' is defined as follows:

$$r' = -r'_0 \cdot e^{(\theta - \theta_0) \tan \varphi} \tag{17}$$

The ratio r'_0/r_0 reaches zero when C'D' reduces to the point O. With the log-spirals r and r' defining the failure mechanism, the distance r_m between the rotation centre O and the centre of the rotating circle and the radius R of the rotating circle are defined as follows:

$$\begin{cases} r_m = \frac{r+r'}{2} \\ R = \frac{r-r'}{2} \end{cases} \tag{18}$$

To calculate the work rate of the failure mechanism, a local coordinate system (x, y) is adopted, as shown in Figure 4. (Axis x is perpendicular to the symmetric plane of the failure mechanism). And the shaded area in the (x, y) coordinate system represents one cross section of the failure block in the weak layer.

The infinitesimal elementary volume is calculated as follows:

$$dV = dxdy(r_m + y)d\theta (19)$$

Thus, according to the Eq. (3), the work rate of the soil weight can be obtained as follows:

$$W_G = 2\omega\gamma \int_{\theta_0}^{\theta_h} \int_0^{x^*} \int_a^{y^*} (r_m + y)^2 dy dx d\theta$$
 (20)

where

$$\begin{cases} x^* = \sqrt{R^2 - a^2} \\ y^* = \sqrt{R^2 - x^2} \end{cases}$$

where a is a function of θ , as follows:

$$a = r_0 \frac{\cos \theta_0}{\cos \theta} - r_m$$

The infinitesimal elementary area is calculated as follows:

$$dS = Rdt \cdot (R\cos t + r_m)d\theta \cdot \frac{1}{\cos \theta}$$
 (21)

Thus, according to the Eq. (2), the dissipation along the discontinuity surface is obtained as follows:

$$W_D = 2c\omega \int_{\theta_D}^{\theta_h} \int_{0}^{t^*} R(R\cos t + r_m)^2 dt d\theta$$
 (22)

Where t^* is described as follows:

$$t^* = \arccos\left(\frac{a}{R}\right)$$

where t is shown in Figure 4. Michalowski and Drescher [24] provided a simpler method for calculating the dissipation of the failure mechanism in cohesive-frictional soil, and more details can be found in that work (this method is confined to the soil with a non-zero friction angle φ). It is noted that the calculation for dissipation in this paper can be used for both cohesive-frictional and purely cohesive soils. The calculation can simply transform into the formula for purely cohesive soils when $\varphi = 0$.

The infinitesimal elementary area along the interface *CD* is calculated as follows:

$$dS = R \sin t^* \cdot \frac{r_0 \cos \theta_0}{\cos \theta} d\theta \cdot \frac{1}{\cos \theta}$$
 (23)

According to the Eqs. (4) and (5), the work rates done by the slurry pressure and water pressure are respectively calculated as follows:

$$W_{sr} = 2\gamma_{sr}\omega \int_{\theta_0}^{\theta_h} \left(R^2 - a^2\right)^{0.5} \frac{r_0^2 \cos^2 \theta_0}{\cos^2 \theta} \tan \theta (h_1$$
 (24)

$$+r_0\cos\theta_0\tan\theta-r_0\sin\theta_0)d\theta$$

$$W_{W} = 2\gamma_{W}\omega \int_{\theta_{0}}^{\theta_{h}} \left(R^{2} - a^{2}\right)^{0.5} \frac{r_{0}^{2}\cos^{2}\theta_{0}}{\cos^{2}\theta} \tan\theta (h_{2})$$
 (25)

$$+r_0\cos\theta_0\tan\theta-r_0\sin\theta_0$$
) $d\theta$

In the search for the minimum of the safety factor F, the ratio r_0'/r_0 , θ_0 and θ_h are the independent variable parameters. Moreover, the failure mechanism must be subjected to an independent constraint on the length B of slurry trench, because the failure mechanism tends to increase the range of the failure zone during the process of minimizing the safety factor F infinitely if no constraints are placed on the length of the mechanism.

3 Numerical Simulation

This section presents a study of numerical method on the local stability of a slurry trench. And the results of numerical simulation will be compared with the proposed analytical method. In this numerical model, the detailed information about the geologic and geometric conditions is summarized in Table 1 and the soil profile is shown in Figure 5.

Figure 6 presents a half part of a slurry trench, it is easily found that the slurry trench has an advantage of symmetry along two axes. So this paper takes a quarter of the slurry trench model to study. Three layers are built in the

894 — W. Li and C. Zhang DE GRUYTER

Table 1: Geologic parameters

Layer	Туре	Unit Weight (kN/m³)	E _s (MPa)	Cohesion (kPa)	Friction angle (°)	Poisson ratio <i>v</i>
1	Silty clay	20.0	7.2	45	17	0.4
2	Sand	20.0	14.4	5	20	0.4
3	Silty clay	20.0	9.8	45	17	0.4

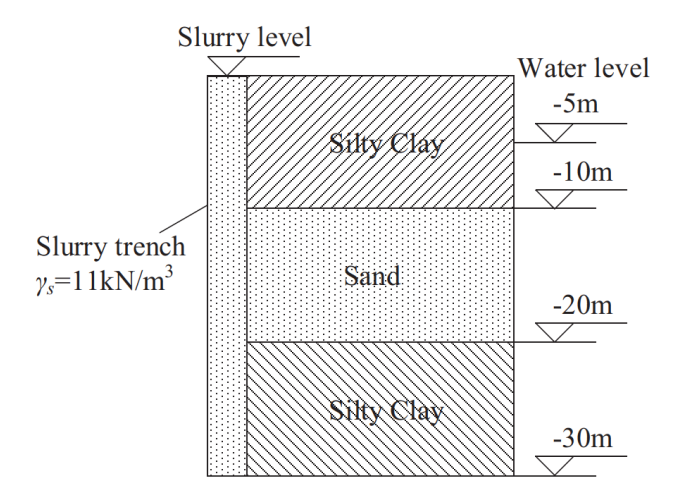


Figure 5: Soil profile of the slurry trench.

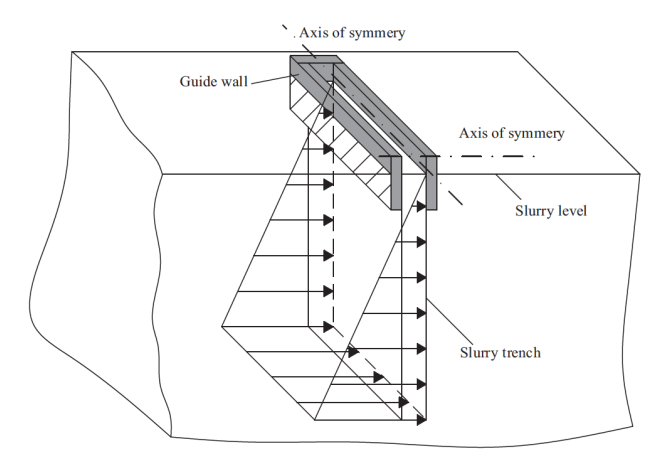


Figure 6: Schematic of a slurry trench model.

numerical model, and a weak soil is sandwiched between two stiff soils, as shown in Figure 7. The numerical model is established with a discretization of 12000 zones and a total of 14091 nodes. The size of the numerical model is 10m in the X direction, 30m in the Z direction and 5m in the Y direction (the length B of trench is 10m). The boundary conditions are set as follows: Nodes at the bottom of mesh are fully fixed. Nodes on the vertical symmetric plane are only fixed in the X direction. And Nodes on the vertical boundary are only free to move vertically. The load distribution due to the slurry pressure acting on the trench face

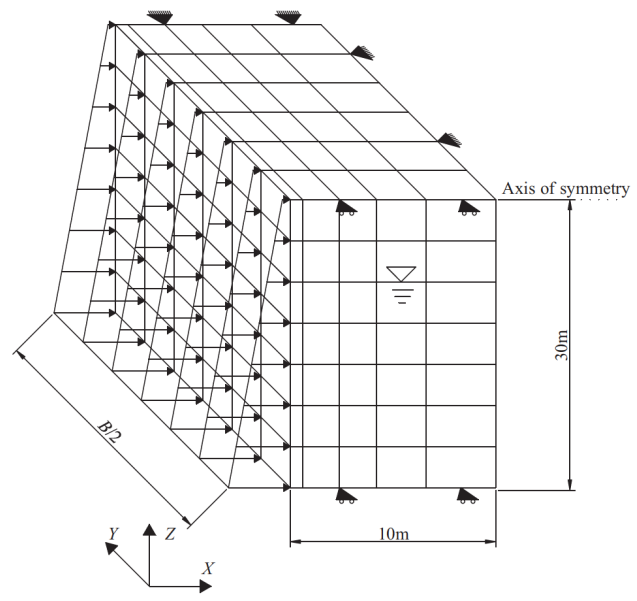


Figure 7: Numerical model of a slurry trench in FLAC3D.

is converted into the equivalent nodal force in the FLAC 3D model. And a hydrostatic stress field is set up in the model. An elastic-perfectly plastic constitutive model governed by the Mohr-Coulomb criterion is assigned to the soil. In addition, the guide wall is simply modelled by preventing the nodes representing the guide wall from the movement in the *X* direction.

In this numerical analysis, the safety factor is determined with the strength reduction method (SRM). The soil strength parameters of the weak soil are defined as follows:

$$\begin{cases} c_F = \frac{c}{F} \\ \varphi_F = \arctan\left(\frac{\tan\varphi}{F}\right) \end{cases}$$
 (26)

The initial values of the safety factor F is provided with 0.1, which gives the high values of the strength parameters and the weak layer will be in the elastic condition. The safety factor F is then incrementally increased by 0.01 and the strength of weak layer is continuously reduced. The process is repeated until the failure occurs at the sandwiched soil layer (In FLAC 3D, a monitor point is set on the midpoint of weak layer. And the failure occurs when the displacement of the monitor point has a sudden

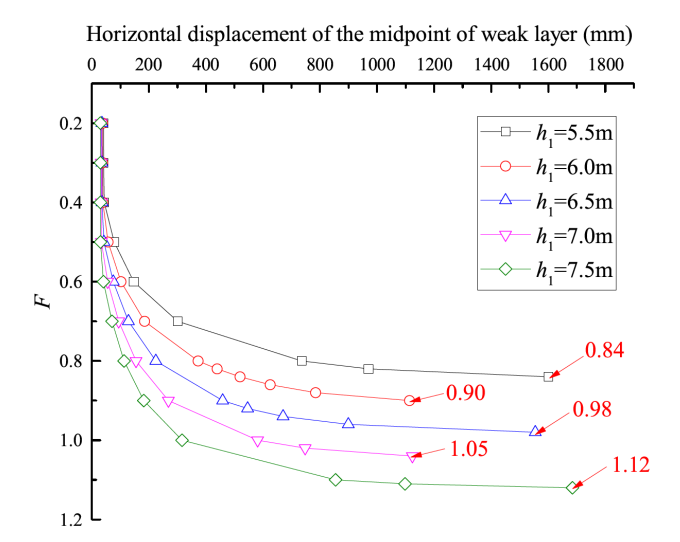


Figure 8: Determination on the safety factor of the weak layer in FLAC3D.

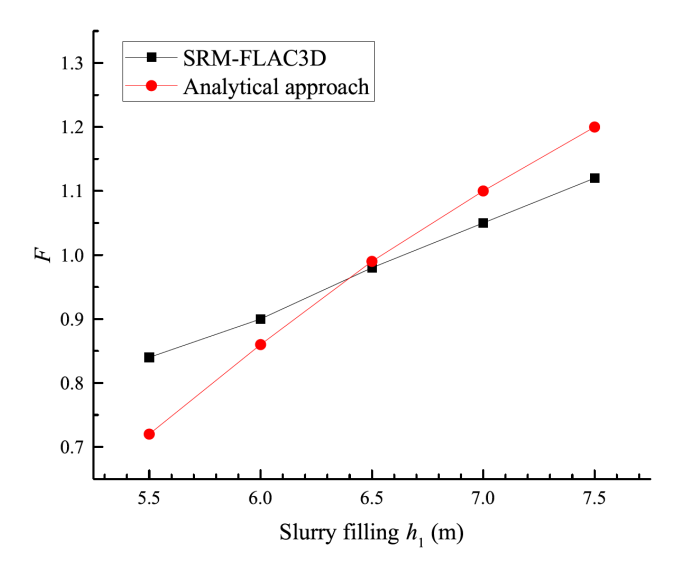


Figure 9: Comparison of the safety factors obtained from analytical approach and SRM-FLAC3D.

increase). At this instant, the value of the safety factor *F* comes to be the minimal safety factor of local stability of a slurry trench, as shown in Figure 8.

4 Results and Discussion

This section will present the results obtained from the analytical method and the numerical simulation. Both the safety factor *F* and the failure pattern of the analytical method will be compared with that of the numerical simulation. Besides, the influences of the geologic and geometric parameters on the safety factor will be investigated.

4.1 Comparison between the Numerical Simulation and the Analytical Method

In this section, the results of the proposed failure mechanism for a slurry trench in the cohesive-frictional soils will be compared with that of the numerical simulation.

Figure 9 presents the comparison between the SRM defined safety factors obtained from the numerical simulation and the load-resisting ratio defined safety factors calculated by the proposed kinematical analytical solution. It is noted that the lines representing respectively the numerical results and the analytical solutions intersects at the point where the safety factor is equal to 1.0. Before this point, the safety factors obtained from the analytical approach are smaller than that of the SRM-FLAC3D. Beyond this point, the SRM-FLAC3D gives a more conservative result. For the most practical cases, the engineering projects are considered to be safe when the F is larger than one, and the projects are believed to be dangerous or have a risk of failure when the *F* is smaller than one. Therefore, it is suggested that the engineers should take the results of the analytical approach and the SRM-FLAC3D simultaneously into consideration in different cases and choose a more secure way to determine the safety factor of the local stability of a slurry trench. Besides, it is shown that two methods give the same estimate on whether the slurry trench is safe or not, thus the local stability of a slurry trench can be assessed by the SRM-FLAC3D and analytical approach in the meantime.

Figure 10 shows the comparison of the failure patterns predicted by the proposed failure mechanism and the contour of shear strain increment of FLAC3D in the vertical symmetric plane. The proposed failure mechanism is assumed to be confined to the sand layer sandwiched by two strong soils. The contour of shear strain increment of FLAC3D shows the zone where shear strain appears, and the zone of large shear strain is also regarded as the region where the shear failure occurs. It can be seen from Figure 10 that the large shear appears around the curve plotted by the analytical method. Consequently, the comparison shows the predicted discontinuity surface agrees well with the zone where large shear strain appears, which proves the discontinuity surface predicted by the analytical approach is reasonable and the local failure of a slurry trench occurs in the vicinity of the trench face of the weak layer.

Figure 11 shows the comparison of the failure patterns predicted by the proposed failure mechanism and the plastic zone obtained from FLAC3D in the vertical symmetric plane. It can be seen that the plastic zone of FLAC3D agrees well with the failure pattern of the analytical method. The

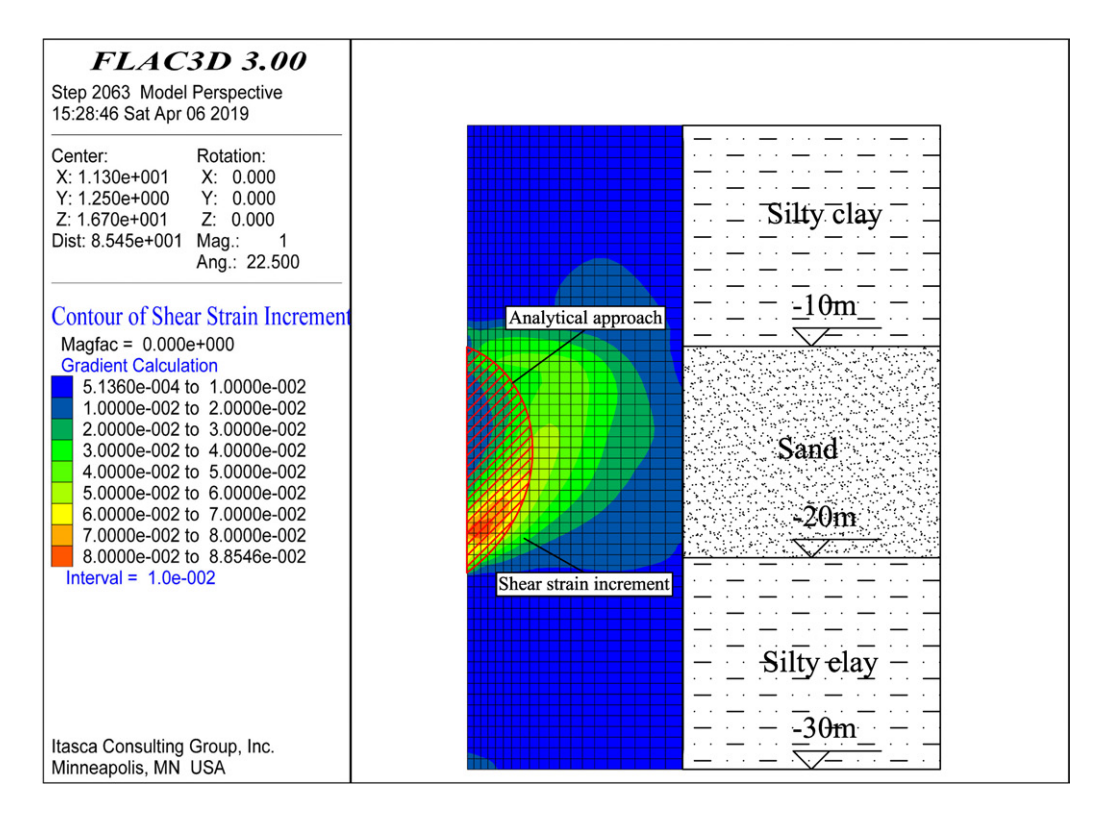


Figure 10: Comparison between the predicted discontinuity surface and the contour of shear strain increment of FLAC3D in the symmetric (x, z) plane.

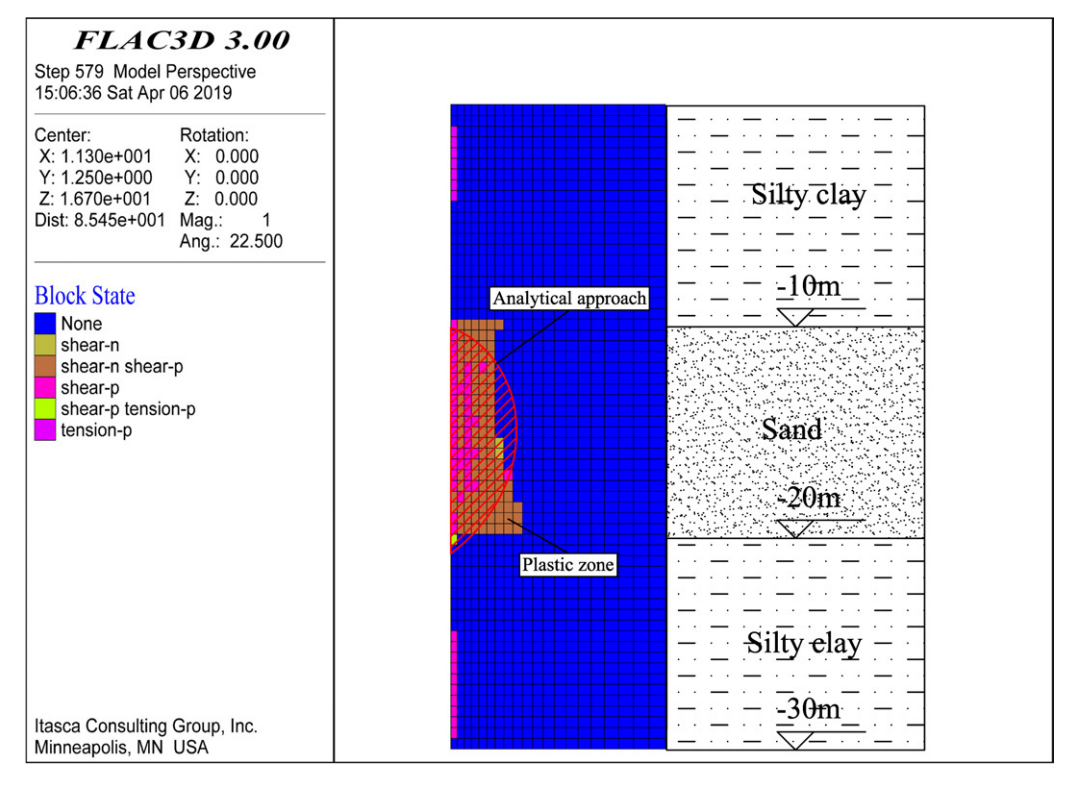
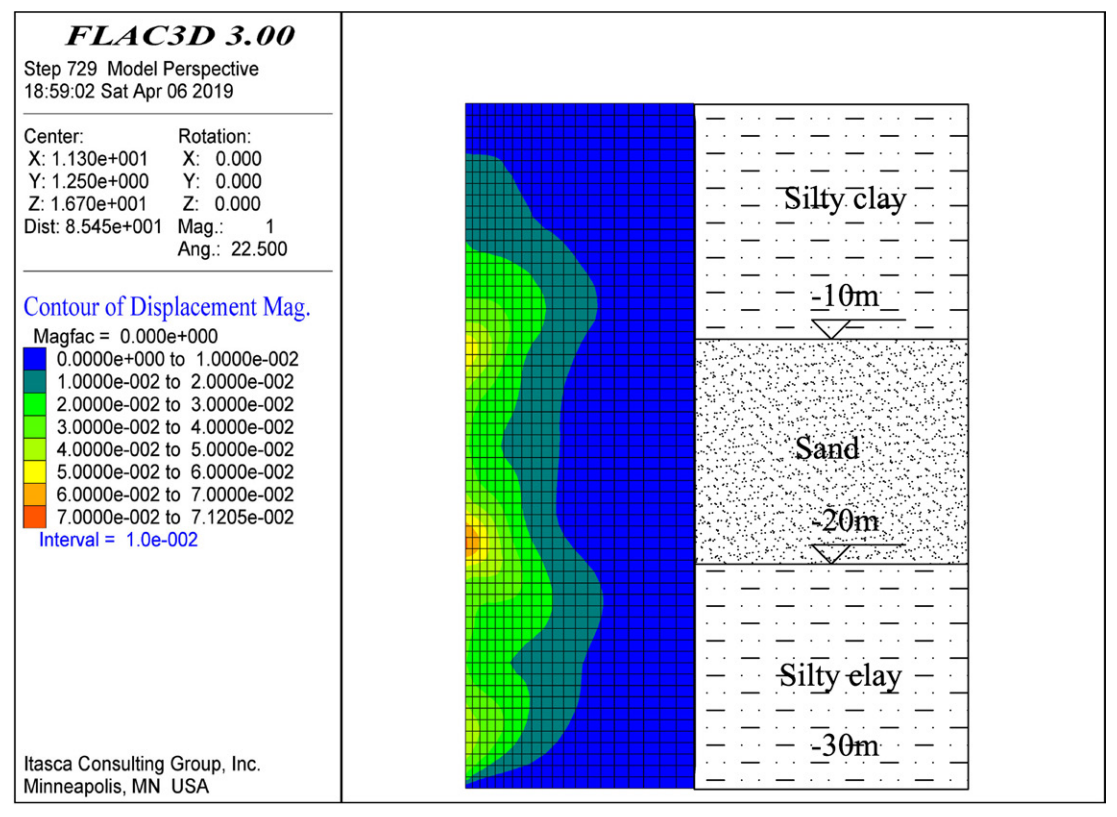


Figure 11: Comparison between the predicted discontinuity surface and the plastic zone of FLAC3D in the symmetric (x, z) plane.



(a)

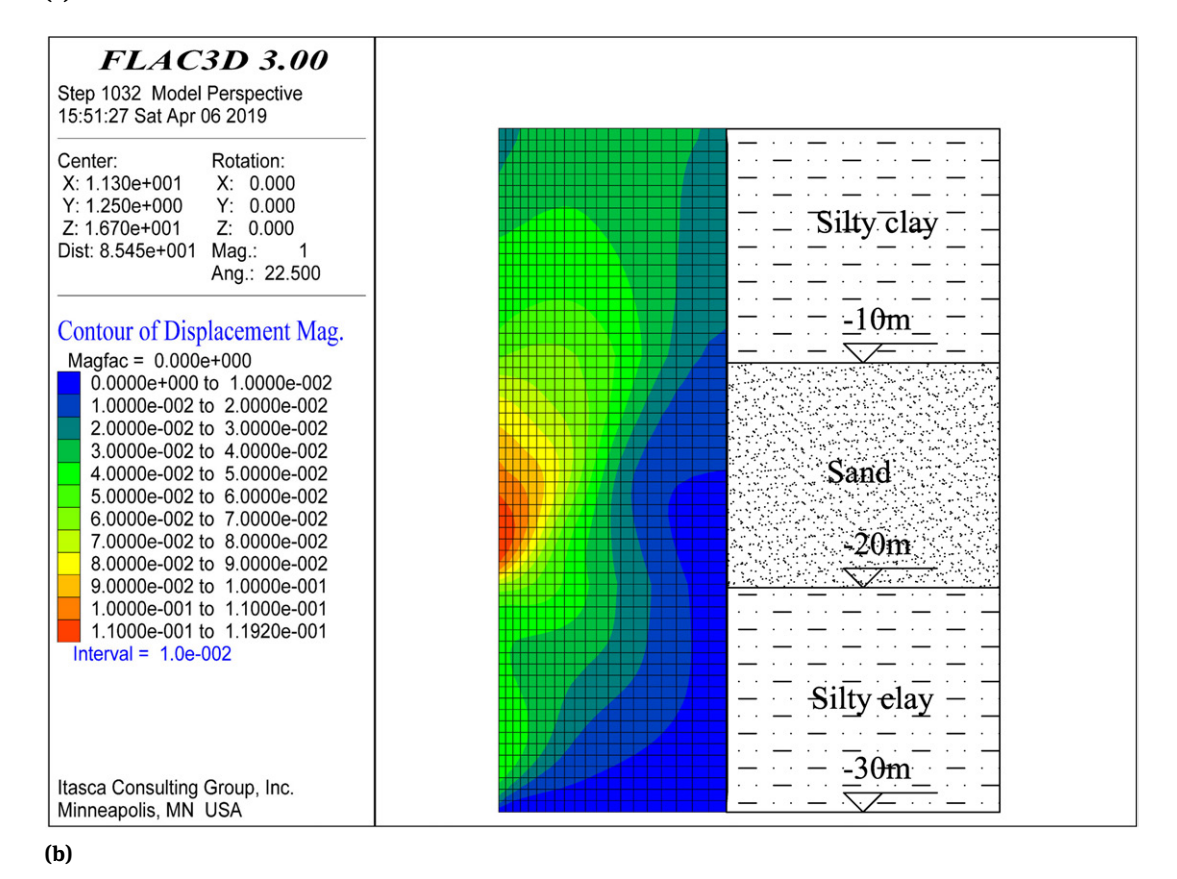


Figure 12: Local failure process of the weak layer in FLAC3D: (a) Initial stage; (b) Terminal stage; (c) Fall-off.

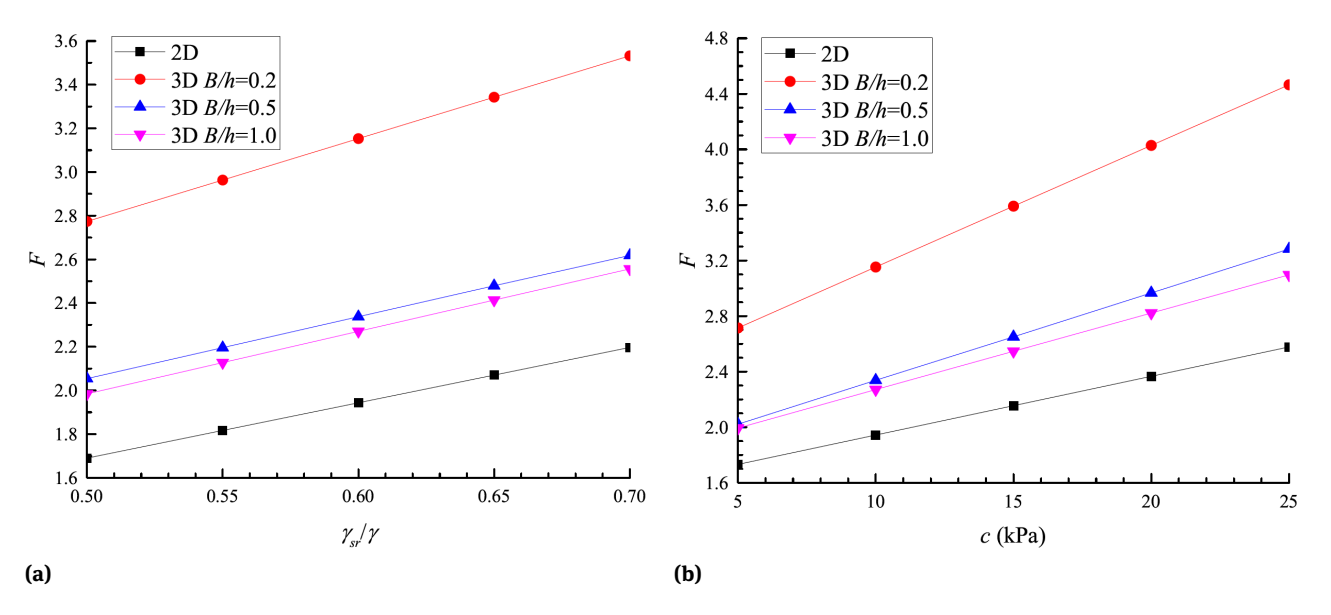


Figure 13: Influence of the geologic parameters on the safety factor (c = 10kPa, $\varphi = 10$, $\gamma = 20$ kN/m³, $\gamma_{sr}/\gamma = 0.6$, h = 10m, $h_1 = 5$ m, $h_2 = 0$ m): (a) γ_{sr}/γ ; (b) ϵ ; (c) φ .

plastic zone first occurs at two interfaces between the stiff soil and the sandwiched weak soil. And then the plastic zone extends in the sandwiched weak soil in a logarithmic spiral surface similar with the 3D failure mechanism proposed in this paper. At last, the plastic zone will develop throughout the whole weak soil layer and the local failure of the slurry trench happens.

Figure 12 shows the local failure process of a slurry trench. At the initial stage, it can be seen from the Figure 12(a) that the displacement of two interfaces between sand and silty clay is larger than other zones. It shows that the local failure of a slurry trench initiates at the upper and lower boundaries of the weak layer. And then the local failure develops inside the weak layer and gradually propagates to the middle zone of the weak layer. Finally the local failure occurs when the upper and lower failure zones connect and the whole weak layer is intersected, as shown in Figure 12(b). After the local failure of a slurry trench, the failure soil inside the weak layer will be extruded by the gravity of the overlying soil. As a result, the failure soil falls off from the trench face, as shown in Figure 12(c). It is interesting to find that the situation of Figure 12(c) is similar with that shown in Figure 1.

4.2 Influences of the Geologic and Geometric Parameters on the Local Stability

In this section, the parametric studies of the safety factor F in 3D and 2D analyses of a slurry trench are presented. The influence investigations of the geometric and geologic parameters of a slurry trench on the safety factors F are conducted.

Figure 13 shows the curves of the safety factor F versus different geologic parameters. It is shown that the 3D safety factors increase with the increase of the ratio γ_{ST}/γ , cohesion c and friction angle φ , but decrease with the increase of the ratio B/h and converge to the minima of the safety factors, which are approximately 1.2 times greater than that of 2D analyses in three cases. The increase of the slurry density can directly increase the safety factor F. Moreover, it can be seen that the influences of the friction angle φ on the safety factor are obviously greater than that of the cohesion c, which suggests that the friction angle φ of the soil plays a more important part in improving the local stability of a slurry trench in cohesive-frictional soils.

Figure 14(a) presents the curves of the safety factor F versus the thickness h of the weak layer. The safety factor decreases with the increase of the thickness h of the weak layer. It is shown that the thickness h has a great impact on the safety factor F of the local stability. But with the increase of the thickness h, the decline rate of the safety factor gradually decreases. Figure 14(b) shows the curves of the safety factor F versus the ratio B/h with different thick-

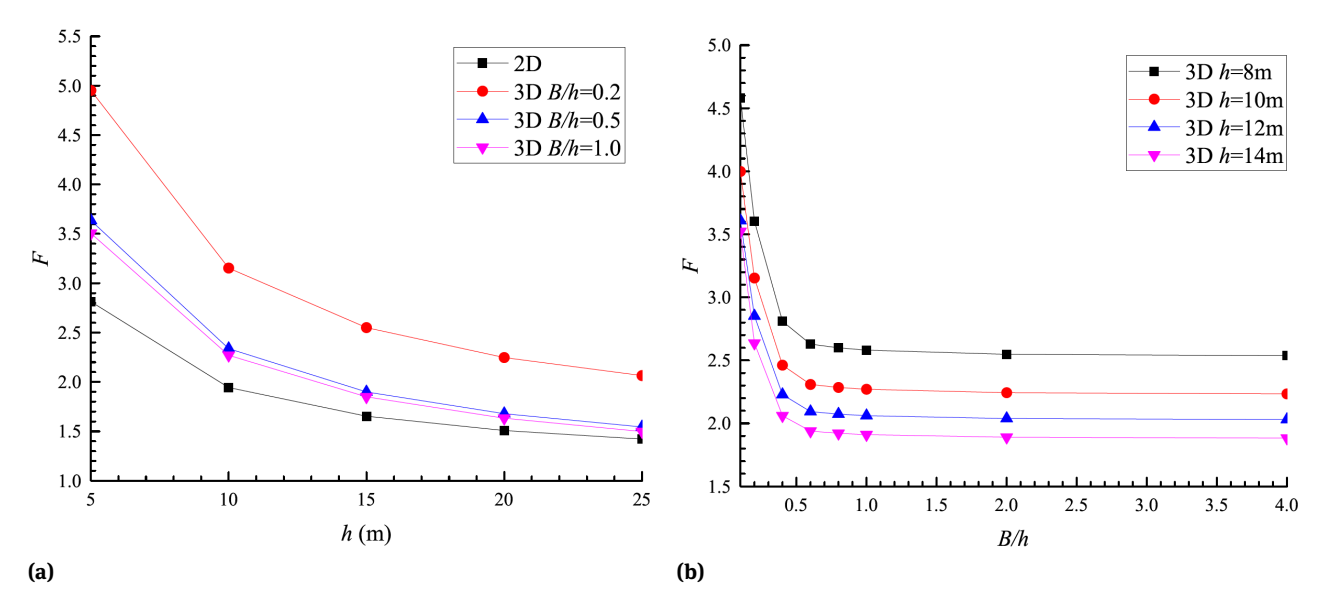


Figure 14: Influence of geometric parameters on the safety factor (c = 10kPa, $\varphi = 10$, $\gamma = 20$ kN/m³, $\gamma_{sr}/\gamma = 0.6$, $h_1 = 5$ m, $h_2 = 0$ m): (a) h_3 ; (b) B/h_2 .

ness h. It can be seen that the safety factors is closely related with the ratio B/h. The safety factors rapidly converge to constant values with the increase of the ratio B/h, which was also mentioned by Duncan [30] and Michalowski and Drescher [28]. Thus the 3D safety factor is only suitable for the slurry trench with a limited length B in the third dimension. When the length B of the slurry trench is large, the 2D safety factor will give a more appropriate estimate on the local stability of a slurry trench.

5 Conclusions

The 2D and 3D rotational failure mechanisms for the local stability of the slurry trench in cohesive-frictional soils are presented in this paper. The upper solutions of the safety factors of the local stability are obtained through a theoretical derivation based on the kinematic method of the limit analysis. Moreover, a numerical simulation is performed to investigate the local stability of the slurry trench and verify the effectiveness and reasonability of the analytical solution. Finally, a parametric study is carried out to study the influences of the geometric and geologic parameters on the safety factor. The main conclusions are as follows:

1. The 2D local failure mechanism of the slurry trench in a weak soil sandwiched by two stiff soils is defined by a log-spiral. For the 3D local failure mechanisms of the slurry trench, the failure surfaces has a horn shape with an apex angle 2φ . The vertical symmet-

- ric plane is defined by two log-spirals, and the whole mechanism is generated by rotating a circle with increasing diameter.
- 2. A numerical method combined with the strength reduction technique is performed to study the local stability of the slurry trench. The local failure process of a slurry trench is summarized. The safety factors predicted by the numerical method and the solution of the analytical method give the same estimate on the safety of the slurry trench, and the local failure pattern obtained from analytical method corresponds with that of the numerical simulation, which verifies that the proposed analytical solution is effective and reasonable. It is suggested that the results of the analytical approach and SRM-FLAC3D should be taken into account simultaneously to study the local stability of a slurry trench
- 3. For the geologic parameters, the safety factors increase with the increase of the ratio γ_{sr}/γ , the friction angle φ and the cohesion c. The increase of the slurry density γ_{sr} can directly increase the safety factor. The influences of the friction angle φ on the safety factor are greater than that of the cohesion c, which plays a more important part in improving the local stability of a slurry trench in cohesive-frictional soils.
- 4. For the geometric parameters, the safety factors decrease with the increase of the thickness of weak layer *h* and the ratio of *B/h*. But the decline rate of safety factor will gradually decrease with the in-

crease of the thickness h. The safety factors rapidly converge to the constant values with the increase of the ratio B/h, thus the 3D safety factor is only suitable for the slurry trench with a limited length B. When the length B of the slurry trench is large, the 2D safety factor will give a more appropriate estimate.

Acknowledgement: The authors acknowledge the financial support provided by Beijing Municipal Natural Science Foundation of China (Grant No.8172037) and the National Natural Science Foundation of China (Grant No.51978042)

References

- Oblozinsky P., Ugai K., Katagiri M., Saitoh K., Ishii T., Masuda T., et al., A design method for slurry trench wall stability in sandy ground based on the elasto-plastic FEM. Comput. Geotech., 2001, 28(2), 145-159.
- Stolle D., Guo P., Limit equilibrium slope stability analysis using rigid finite elements. Can. Geotech. J., 2008, 45(5), 653-662.
- Srivastava A., Babu G., Haldar S., Influence of spatial variability of permeability property on steady state seepage flow and slope stability analysis. Eng. Geol., 2010, 110(3), 93-101.
- Xu J., Debris slope stability analysis using three-dimensional finite element method based on maximum shear stress theory. Environ. Earth. Sci., 2011, 64(8), 2215-2222.
- Tsai J.S., Chang J.C., Three-dimensional stability analysis for slurry-filled trench wall in cohesionless soil. Can. Geotech. J., 1996, 33(5), 798-808.
- Tsai J.S., Jou L.D., Hsieh H.S., A full-scale stability experiment on a diaphragm wall trench. Can. Geotech. J., 2000, 37(2), 379-392.
- Fox P.J., Analytical solutions for stability of slurry trench. J. Geotech. Geoenviron., 2004, 130(7), 749-758.
- Li Y.C., Pan Q., Cleall P.J., Chen Y.M., Ke H., Stability analysis of slurry trenches in similar layered soils. J. Geotech. Geoenviron., 2013, 139(12), 2104-2109.
- Jin X.F., Liang S.T., Zhu X.J., Stability of Three-Dimensional Slurry Trenches with Inclined Ground Surface: A Theoretical Study. Adv. Mater. Sci. Eng., 2015(6), Article ID: 362160.
- [10] Xiao H., Sun Y., Global and local stability analysis of slurry trenches under surcharge in soft soils. Int. J. Geotech. Eng., 2016, 10(2), 205-211.
- [11] Zhang F., Gao Y.F., Leshchinsky D., Zhu D.S., Lei G.H., Threedimensional stability of slurry-supported trenches: End effects. Comput. Geotech., 2016, 74, 174-187.
- [12] Han C.Y., Wang J.H., Xia X.H., Chen J.J., Limit analysis for local and overall stability of a slurry trench in cohesive soil. Int. J. Geomech., 2012, 15(5), 06014026.

- [13] Han C.Y., Chen J.J., Wang J.H., Xia X.H., 2D and 3D stability analysis of slurry trench in frictional/cohesive soil. J. Zhejiang. Uni-SC A., 2013, 14(2), 94-100.
- [14] Tsai J.S., Stability of weak sublayers in a slurry supported trench. Can. Geotech. J., 1997, 34(2), 189-196.
- [15] Tsai J.S., Chang C.C., Jou L.D., Lateral extrusion analysis of sandwiched weak soil in slurry trench. J. geotech. Geoenviron. Eng., 1998, 124(11), 1082-1090.
- [16] Shen C., Zhou S.H., Local Stability of Slurry Trench in Sandwiched Sand Layer with Confined Water Pressure. International Conference on Transportation Engineering, Chengdu, China. 2013, 2540-2548.
- [17] Michalowski R.L., Limit analysis and stability charts for 3D slope failures. J. Geotech. Geoenviron. Eng., 2010, 136(4), 583-593.
- [18] Kumar J., Sahoo J.P., Upper bound solution for pullout capacity of vertical anchors in sand using finite elements and limit analysis. Int. J. Geomech., 2012, 12(3), 333-337.
- [19] Leca E., Dormieux L., Upper and lower bound solutions for the face stability of shallow circular tunnels in frictional material. Géotechnique, 1990, 40(4), 581-606.
- [20] Soubra A.H., Kinematical approach to the face stability analysis of shallow circular tunnels. 8th International Symposium on Plasticity, Vancouver, Canada, 2002, 443-445.
- [21] Subrin D., Wong H., Tunnel face stability in frictional material: a new 3D failure mechanism. Comptes Rendus Mecanique, 2002, 330(7), 513-519.
- [22] Mollon G., Dias D., Soubra A.H., Probabilistic analysis and design of circular tunnels against face stability. Int. J. Geomech., 2009, 9(6), 237-249.
- [23] Li W., Zhang C.P., Zhang X., Stability analysis of the tunnel face in the cohesive-frictional soils considering the arch effect and rotational mechanism. J. Chin. Inst. Eng., 2018, 41(8): 697-709.
- [24] Han K.H., Zhang C.P., Zhang D.L., Upper-bound solutions for the face stability of a shield tunnel in multilayered cohesive-frictional soils. Comput. Geotech., 2016, 79:1-9.
- [25] Zhang C.P., Han K.H., Zhang D.L., Face stability analysis of shallow circular tunnels in cohesive-frictional soils. Tunn. Undergr. Sp. Tech., 2015, 50:345-357.
- [26] Li W., Zhang C.P., Zhu W.J., Zhang D.L., Upper-bound solutions for the face stability of a non-circular NATM tunnel in clays with a linearly increasing undrained shear strength with depth. Comput. Geotech., 2019, 114, 103136. DOI: 10.1016/j.compgeo.2019.103136.
- [27] Li W., Zhang C.P., Face Stability Analysis for a Shield Tunnel in Anisotropic Sands. Int. J. Geomech., 2019, doi: 10.1061/(ASCE)GM.1943-5622.0001666.
- [28] Michalowski R.L., Drescher A., Three-dimensional stability of slopes and excavations. Géotechnique, 2009, 59(10), 839-850.
- [29] Anthoine A., Mixed modelling of reinforced soils within the framework of the yield design theory. Comput. Geotech., 1989, 7(1),
- [30] Duncan J.M., State-of-the-art: limit equilibrium and finite element analysis of slopes. J. Geotech. Eng. Div., 1996, 122(7), 577-596.